Acta Cryst E CRYSTALLOGRAPHIC COMMUNICATIONS

ISSN 2056-9890

Structural, Hirshfeld and DFT studies of conjugated *D*–π–*A* carbazole chalcone crystal

Muhamad Fikri Zaini,[a] Ibrahim Abdul Razak,[a] Wan Mohd Khairul[b] and Suhana Arshad[a]*

[a]X-ray Crystallography Unit, School of Physics, Universiti Sains Malaysia, 11800 USM, Penang, Malaysia, and [b]School of Fundamental Science, Universiti Malaysia Terengganu, 21030, Kuala Terengganu, Terengganu, Malaysia. *Correspondence e-mail: suhanaarshad@usm.my

Received 23 December 2019
Accepted 12 February 2020

Edited by J. Ellena, Universidade de São Paulo, Brazil

Keywords: carbazole chalcone; crystal structure; Hirshfeld surface; DFT; molecular electrostatic potential.

CCDC reference: 1967669

Supporting information: this article has supporting information at journals.iucr.org/e

A new conjugated carbazole chalcone compound, (*E*)-3-[4-(9,9a-dihydro-8a*H*-carbazol-9-yl)phenyl]-1-(4-nitrophenyl)prop-2-en-1-one (CPNC), $C_{27}H_{18}N_2O_3$, was synthesized using a Claisen–Schmidt condensation reaction. CPNC crystallizes in the monoclinic non-centrosymmetric space group *Cc* and adopts an *s-cis* conformation with respect to the ethylenic double bonds (C=O and C=C). The crystal packing features C—H···O and C—H···π interactions whose percentage contribution was quantified by Hirshfeld surface analysis. Quantum chemistry calculations including geometrical optimization and molecular electrostatic potential (MEP) were analysed by density functional theory (DFT) with a B3LYP/6–311 G++(d,p) basis set.

1. Chemical context

Chalcone is a privileged structure comprising two aromatic rings that are linked by a three-carbon α,β-unsaturated carbonyl system. Chalcones demonstrate wide-ranging biological activities such as anti-inflammatory and anticancer (Cui *et al.*, 2008; Srinivasan *et al.*, 2009; Wang *et al.*, 2013) and have applications in non-linear optics (Zaini, Arshad *et al.*, 2019). They are currently attracting considerable attention because they offer an excellent π-conjugated system within the double bond at the ethylenic bridge (Teo *et al.*, 2017). Furthermore, the conjugated chalcone could be enhanced with appropriate electron-pulling and electron-pushing functional groups on the benzene rings (Zhuang *et al.*, 2017). The increased involvement of donor and acceptor interactions in the molecule improves the molecular charge transfer and degree of non-linearity (Davanagere *et al.*, 2019). The high planarity and presence of stable *E* isomer in the solid state stabilizes the crystal structure (Custodio *et al.*, 2020).

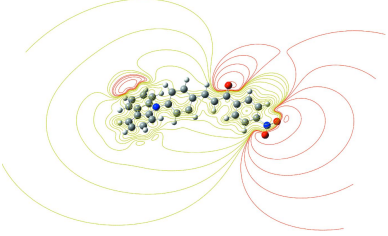

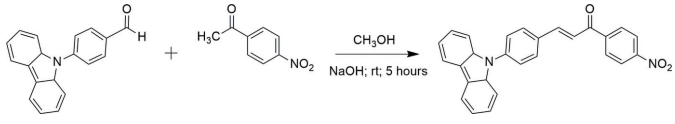

In a continuation of our studies (Zaini *et al.*, 2018; Zaini, Razak *et al.*, 2019), we report herein the synthesis and structural properties of the conjugated carbazole chalcone system of (*E*)-3-[4-(9,9a-dihydro-8a*H*-carbazol-9-yl)phenyl]-1-(4-nitrophenyl)prop-2-en-1-one (CPNC). The experimental and theoretical studies and chemical reactivity analysis are discussed.

2. Structural commentary

CPNC is composed of 9-phenylcarbazole and nitrobenzene moieties, which represent donor and acceptor groups, connected by an ethylenic bridge. The molecular and optimized structures of the CPNC with assigned atom-numbering scheme are illustrated in Fig. 1. The geometrical optimization of CPNC was computed with the *Gaussian09W* software package (Frisch *et al.*, 2009) using the DFT method and the B3LYP/6-311G++(d,p) basis set without enforcing any molecular symmetry constraints. There is good agreement between the experimental and optimized structures (see the table in the supporting information), indicating that the basis set used was appropriate in both isolated conditions and the solid-state phase.

CPNC crystallizes in the monoclinic *Cc* space group with four molecules per unit cell. Its molecular structure exhibits an *s-cis* configuration with respect to the ethylenic bridge consisting of carbonyl (C═O; 1.215 (3) Å (experimental), 1.223 Å (DFT)] and carbon–carbon double bond (C═C; 1.320 (3) Å (experimental), 1.348 Å (DFT)]. The CPNC molecule is twisted slightly at the C21—C22 bond, with a C20—C21—C22—C27 torsion angle of −10.4 (3)° (DFT value = −21.3°). The experimental and theoretical C15—C16—C19—C20 torsion angles are 158.6 (3) and 178.8°, respectively. The 9-phenylcarbazole C13—N1 bond is also observed to be twisted [C1—N1—C13—C14 51.8 (4)° (in experimental) and 53.2° (DFT). The small discrepancies in the torsion angles between the experimental and calculated DFT results are caused by the involvement of intermolecular interactions, which are negligible during the optimization process (Arshad *et al.*, 2018).

There is also a twist [dihedral angle = 25.30 (17)°] between the mean planes of the nitrophenyl group [N2/O2/O3/C22–C27; maximum deviation of 0.023 (2) Å at atom O3] and the enone unit [O1/C19–C21; maximum deviation of 0.109 (2) Å at atom C21]. Meanwhile, the enone bridge forms dihedral angles of 31.52 (18) and 21.77 (16)°, respectively, with the C13–C18 phenyl ring and the 9*H*-carbazole unit [N1/C1–C12; maximum deviation of 0.041 (3) Å at atom C2].

The 9*H*-carbazole unit and the C13–C18 phenyl ring subtend a dihedral angle of 53.26 (10)°, which is similar to the dihedral angle of 53.8 (3) between the bridge aromatic ring and the 9*H*-carbazole unit in the related compound 2-[4-(9*H*-carbazol-9-yl)benzylidene]-2,3-dihydroinden-1-one (Kim *et al.*, 2011). The 9*H*-carbazole moiety is nearly co-planar with the nitrobenzene unit, making a dihedral angle of 5.19 (7)° (Fig. 1*c*). This planar nature is possibly due to steric repulsion by the hydrogen atoms of the aromatic rings, leading to a small π-electron delocalization. However, the phenyl ring of the 9-phenylcarbazole moiety subtends a large dihedral angle to the nitrobenzene group of 56.74 (10)° (Fig. 1*d*), which tends to suppress the extension of the conjugation effect through the enone moiety.

3. Supramolecular features

The crystal structure of CPNC is built up in a cluster pattern style where the molecules are linked to each other along the *b*-axis direction *via* C15—H15*A*···O1 interactions (Table 1), as shown in Fig. 2*a*. The tilted distortion of 9-phenylcarbazole ring system is the results of the C18—H18*A*···O2 interaction involving the nitro group, which links the molecules in a head-to-tail arrangement, propagating diagonally along the *ac* direction. Weak C9—H9*A*···*Cg*4 interactions involving the C13-C18 phenyl ring and a carbazole hydrogen of carbazole moiety link the molecules into infinite chains, as depicted in

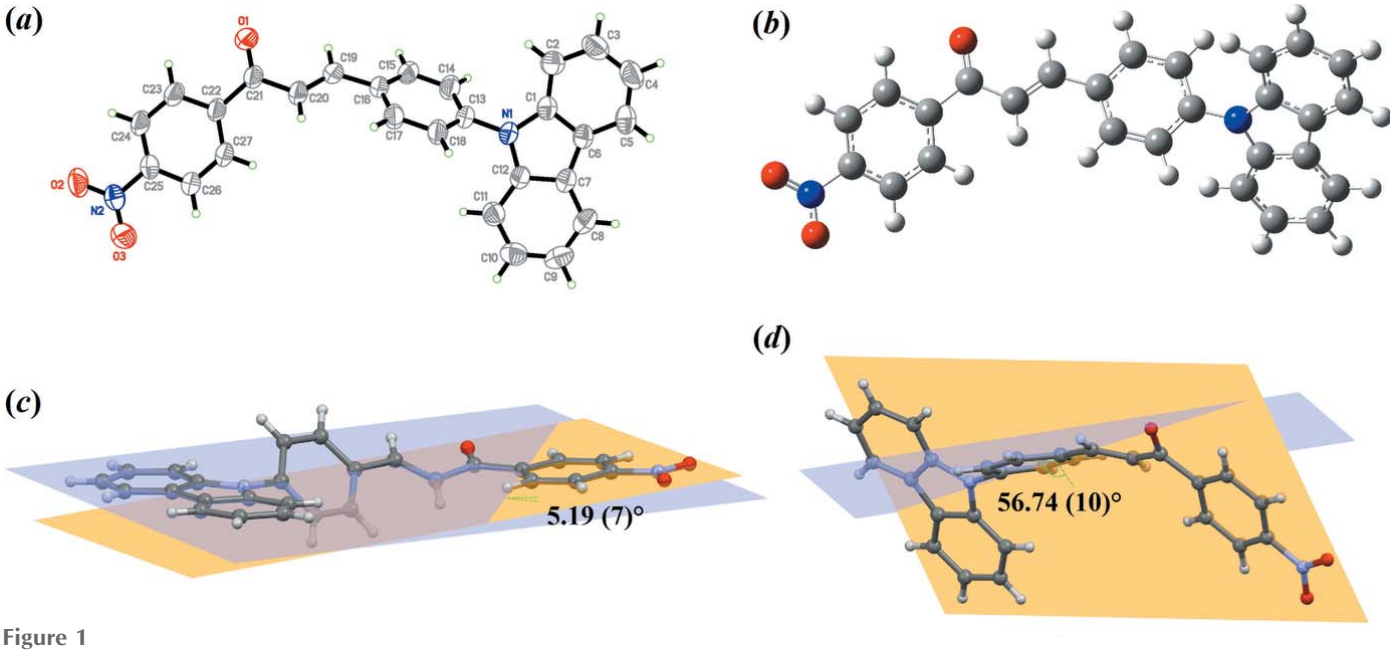

Figure 1
(*a*) The crystal structure of CPNC showing 50% probability ellipsoids, (*b*) the optimized structure, (*c*) the dihedral angle between the nitrobenzene plane and the 9*H*-carbazole unit and (*d*) the dihedral angle between the nitrobenzene plane and the phenyl ring of the 9-phenylcarbazole unit.

Table 1
Hydrogen-bond geometry (Å, °).

*Cg*4 is the centroid of the C13–C18 ring.

D—H···*A*	*D*—H	H···*A*	*D*···*A*	*D*—H···*A*
C15—H15*A*···O1^{i}	0.93	2.42	3.291 (3)	155
C18—H18*A*···O2^{ii}	0.93	2.56	3.490 (3)	173
C9—H9*A*···*Cg*4^{iii}	0.93	2.89	3.758 (3)	155

Symmetry codes: (i) $x, -y+1, z+\frac{1}{2}$; (ii) $x+1, y, z+1$; (iii) $x+\frac{1}{2}, -y+\frac{3}{2}, z+\frac{1}{2}$.

Fig. 2*b*. Overall, the intermolecular C—H···O and C—H···π interactions of CPNC generate a three-dimensional network.

4. Hirshfeld surface analysis

Hirshfeld surface analysis is used to gain a clear understanding of the molecular structure interaction and visualize them graphically. The Hirshfeld surface and related two-dimensional fingerprint plots were generated using *Crystal Explorer3.1* (Wolff *et al.*, 2012). In the d_{norm} surface (Fig. 3), the bright-red spots indicate the involvement of intermolecular C—H···O interactions. The fingerprint plots (Ternavisk *et al.*, 2014) (Fig. 4) indicate the percentage contribution of the H···H, C···H/H···C, O···H/H···O and C···C contacts. The H···H contacts make the largest contribution to the Hirshfeld surface (38.4%) followed by the C···H/H···C contacts (28.2%), which are represented as a pair of characteristic wings. The O···H/H···O (19.1%) contacts display two symmetrical narrow spikes, which confirm the existence of C—H···O interactions. In addition, the presence of weak intermolecular C—H···π interactions can be seen as an orange region marked with black arrows in the shape-index surface (Fig. 5).

5. Molecular electrostatic potential (MEP) analysis

The reactive sites of a molecule can be investigated using molecular electrostatic potential (MEP) analysis (Barakat *et*

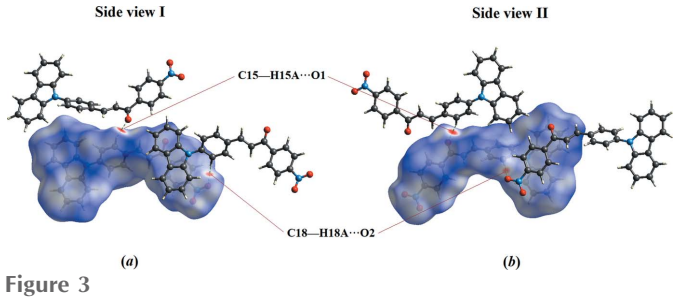

Figure 3
The d_{norm} surfaces showing the intermolecular interactions in CPNC: (*a*) front and (*b*) back.

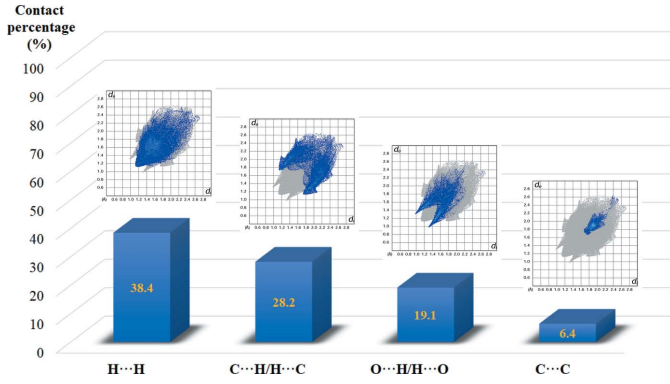

Figure 4
Quantification of different types of contacts and respective fingerprints plots.

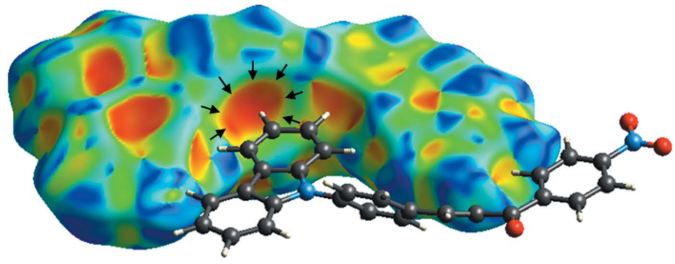

Figure 5
Representation of the C—H···π interactions (indicated by black arrows).

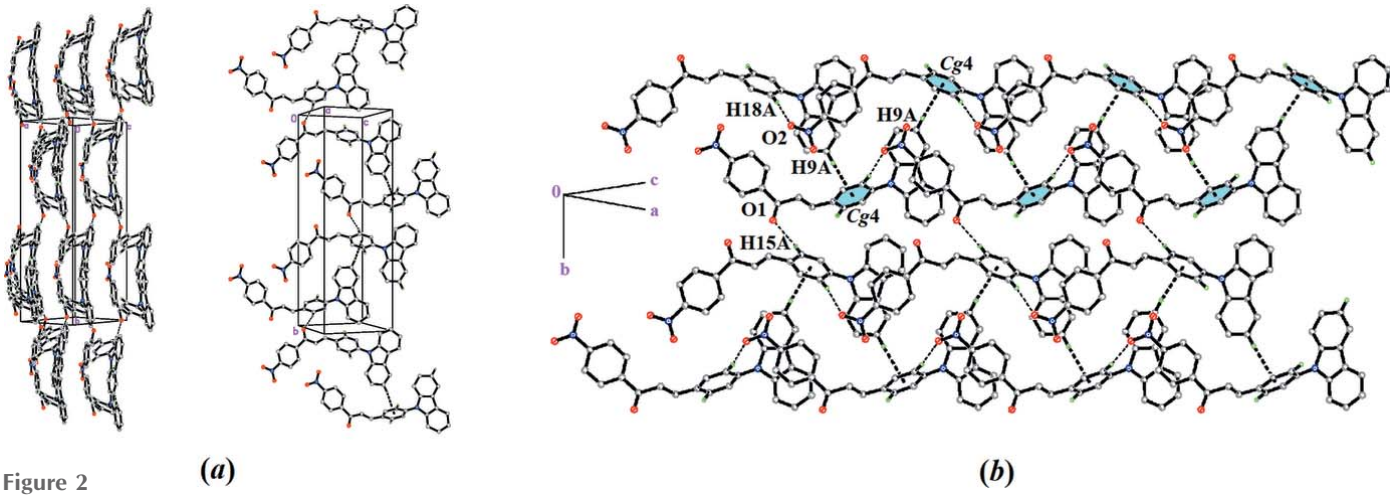

Figure 2
The packing of CPNC showing (*a*) C—H···O and C—H···π interactions (dashed lines) and (*b*) C—H···π interactions forming an infinite chain along the *ac*-plane direction.

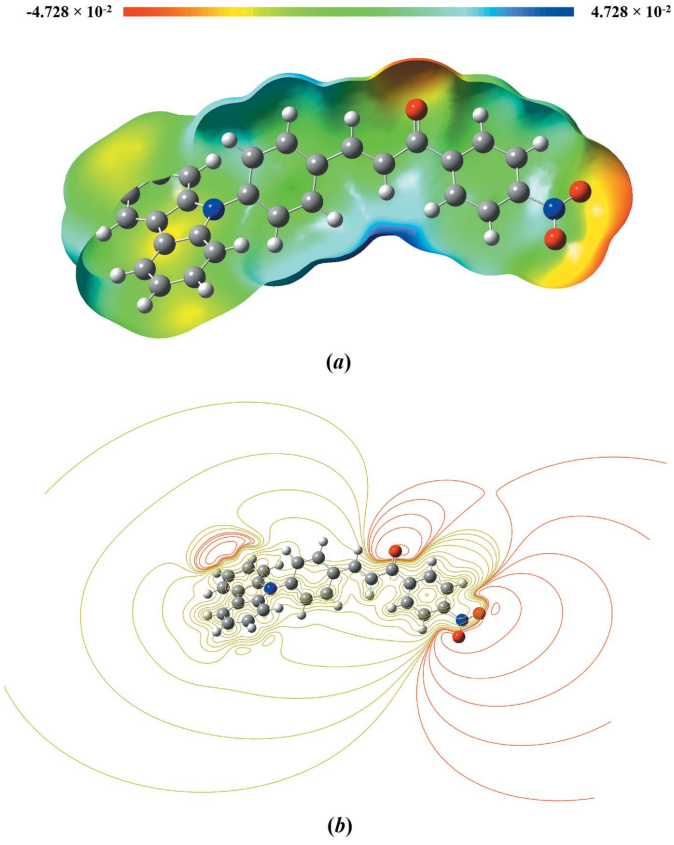

Figure 6
(*a*) Molecular electrostatic potentials (MEP) and (*b*) its contour map mapped on the electron density surface calculated by using the DFT/B3LYP/6–311 G++(d,p) basis set.

Table 2
Experimental details.

Crystal data	
Chemical formula	$C_{27}H_{18}N_2O_3$
M_r	418.43
Crystal system, space group	Monoclinic, *Cc*
Temperature (K)	293
a, *b*, *c* (Å)	9.9690 (5), 24.8828 (15), 8.3049 (4)
β (°)	94.356 (1)
V (Å^3)	2054.13 (19)
Z	4
Radiation type	Mo $K\alpha$
μ (mm^{-1})	0.09
Crystal size (mm)	0.54 × 0.38 × 0.23
Data collection	
Diffractometer	Bruker APEXII CCD
Absorption correction	Multi-scan (*SADABS*; Bruker 2015)
T_{min}, T_{max}	0.783, 0.942
No. of measured, independent and observed [$I > 2\sigma(I)$] reflections	39335, 5995, 5046
R_{int}	0.033
(sin $\theta/\lambda)_{max}$ (Å^{-1})	0.704
Refinement	
$R[F^2 > 2\sigma(F^2)]$, $wR(F^2)$, S	0.041, 0.114, 1.04
No. of reflections	5995
No. of parameters	289
No. of restraints	2
H-atom treatment	H-atom parameters constrained
$\Delta\rho_{max}$, $\Delta\rho_{min}$ (e Å^{-3})	0.19, −0.15
Absolute structure	Flack *x* determined using 2241 quotients $[(I^+)-(I^-)]/[(I^+)+(I^-)]$ (Parsons et al., 2013)
Absolute structure parameter	−0.1 (3)

Computer programs: *APEX2* and *SAINT* (Bruker 2015), *SHELXS97* and *SHELXTL* (Sheldrick, 2008), *SHELXL2014* (Sheldrick, 2015) and *Mercury* (Macrae *et al.*, 2020).

al., 2015). In this study, DFT with the B3LYP/6-311G++(d,p) basis set was utilized to predict the possible location of the nucleophilic and electrophilic attacks. The MEP surface with a colour code from red (−0.04728 a.u) to blue (0.04728 a.u) is depicted in Fig. 6*a*. The carbonyl and nitro groups are nucleophilic (electron-rich) sites in the red-coloured region, while the blue colour indicates the electrophilic (electron-deficient) site localized on the hydrogen atom. These reactive sites are responsible for intermolecular interactions where the red and blue spots suggest the strongest repulsion site (electrophilic attack) and strongest attraction site (nucleophilic attack), respectively. The MEP results are further supported by the electrostatic potential contour map showing the iso-surface lines shown in Fig. 6*b* where the red lines refer to the strong electron-withdrawing atoms such as in carbonyl and nitro substituents.

6. Database survey

A search of the Cambridge Structural Database (CSD, Version 5.40, last update February 2019; Groom *et al.*, 2016) revealed one closely related 9-phenylcarbazole chalcone, namely 1-(anthracen-9-yl)-3-[4-(9*H*-carbazol-9-yl)phenyl]-prop-2-en-1-one (refcode ZIJPUG; Zainuri *et al.*, 2018) with an anthracene system as the ketone substituent. Another similar compound is 2-[4-(9*H*-carbazol-9-yl)benzylidene]-indan-1-one (ISADOW; Kim *et al.*, 2011) in which the 9-phenylcarbazole unit is attached to a 2,3-dihydro-1*H*-inden-1-one moiety. The two crystals were grown by different methods, ZIJPUG by slow evaporation from acetone solution and ISADOW by solvent diffusion using dichloromethane and hexane. The reported molecular structures of ZIJPUG and ISADOW exhibit a π-bridge linker of an enone moiety and the aromatic ring of 9-phenylcarbazole, respectively. Furthermore, the C16—C17—C18—C19 torsion angle in ZIJPUG [−16.4 (3)°] indicates a slight twist, which is which comparable to that in ISADOW [C8—C10—C11—C12 = 178.6 (2)°].

7. Synthesis and crystallization

4′-Nitroacetophenone (5 mmol) and *N*-(4-formylphenyl)-carbazole (5 mmol) were dissolved in 20 mL of methanol and then a catalytic amount of sodium hydroxide solution (5 mL, 20%) was added dropwise under continuous stirring for about 5–6 h at room temperature until a precipitate formed. This was filtered off, washed successively with distilled water and recrystallized from acetone solution, yielding orange block-shaped crystals suitable for X-ray diffraction analysis.

8. Refinement

Crystal data, data collection and structure refinement details are summarized in Table 2. All H atoms were positioned geometrically (C—H = 0.93 Å) and refined using a riding model with U_{iso}(H) = 1.2U_{eq}(C).

Acknowledgements

The authors thank the Malaysian Government and Universiti Sains Malaysia (USM) for the research facilities to conduct this work.

Funding information

The authors thank the Malaysian Government and Universiti Sains Malaysia (USM) for the Research University (RUI) grant No. 1001.PFIZIK.8011081 and the Fundamental Research Grant Scheme (FRGS) No. 203.PFIZIK.6711606.

References

Arshad, S., Zainuri, D. A., Khalib, N. C., Thanigaimani, K., Rosli, M. M., Razak, I. A., Sulaiman, S. F., Hashim, N. S. & Ooi, K. L. (2018). *Mol. Cryst. Liq. Cryst.* **664**, 218–240.

Barakat, A., Al-Majid, A. M., Soliman, S. M., Mabkhot, Y. N., Ali, M., Ghabbour, H. A., Fun, H.-K. & Wadood, A. (2015). *Chem. Cent. J.* **9**, 35.

Bruker (2015). *APEX2*, *SAINT* and *SADABS*. Bruker AXS Inc., Madison, Wisconsin, USA.

Cui, Y., Ao, M., Hu, J. & Yu, L. (2008). *Z. Naturforsch. C.* **63**, 361–365.

Custodio, J. M. F., Guimarães-Neto, J. J. A., Awad, R., Queiroz, J. E., Verde, G. M. V., Mottin, M., Neves, B. J., Andrade, C. H., Aquino, G. L. B., Valverde, C., Osório, F. A. P., Baseia, B. & Napolitano, H. B. (2020). *Arab. J. Chem*. 13, 3362–3371.

Davanagere, H., Jayarama, A., Patil, P. S. G., Maidur, S. R., Quah, C. K. & Kwong, H. C. (2019). *Appl. Phys. A*, **125**, article No.309.

Frisch, M. J., Trucks, G. W., Schlegel, H. B., Scuseria, G. E., Robb, M. A., Cheeseman, J. R., Scalmani, G., Barone, V., Mennucci, B., Petersson, G. A., Nakatsuji, H., Caricato, M., Li, X., Hratchian, H. P., Izmaylov, A. F., Bloino, J., Zheng, G., Sonnenberg, J. L., Hada, M., Ehara, M., Toyota, K., Fukuda, R., Hasegawa, J., Ishida, M., Nakajima, T., Honda, Y., Kitao, O., Nakai, H. & Vreven, T. (2009). *Gaussian 09, Revision B. 01*. Gaussian, Inc., Wallingford, CT, USA.

Groom, C. R., Bruno, I. J., Lightfoot, M. P. & Ward, S. C. (2016). *Acta Cryst.* B**72**, 171–179.

Kim, B.-S., Kim, S.-H., Matsumoto, S. & Son, Y.-A. (2011). *Z. Krist. New Cryst. Struct.* **226**, 177–178.

Macrae, C. F., Sovago, I., Cottrell, S. J., Galek, P. T. A., McCabe, P., Pidcock, E., Platings, M., Shields, G. P., Stevens, J. S., Towler, M. & Wood, P. A. (2020). *J. Appl. Cryst.* **53**, 226–235.

Parsons, S., Flack, H. D. & Wagner, T. (2013). *Acta Cryst.* B**69**, 249–259.

Sheldrick, G. M. (2008). *Acta Cryst*. A**64**, 112–122.

Sheldrick, G. M. (2015). *Acta Cryst*. C**71**, 3–8.

Srinivasan, B., Johnson, T. E., Lad, R. & Xing, C. (2009). *J. Med. Chem.* **52**, 7228–7235.

Teo, K. Y., Tiong, M. H., Wee, H. Y., Jasin, N., Liu, Z.-Q., Shiu, M. Y., Tang, J. Y., Tsai, J.-K., Rahamathullah, R., Khairul, W. M. & Tay, M. G. (2017). *J. Mol. Struct.* **1143**, 42–48.

Ternavisk, R. R., Camargo, A. J., Machado, F. B., Rocco, J. A., Aquino, G. L., Silva, V. H. & Napolitano, H. B. (2014). *J. Mol. Model.* **20**, 2526.

Wang, Z., Wang, N., Han, S., Wang, D., Mo, S., Yu, L., Huang, H., Tsui, K., Shen, J. & Chen, J. (2013). *PLoS One*, **8**, e68566.

Wolff, S., Grimwood, D., McKinnon, J., Turner, M., Jayatilaka, D. & Spackman, M. (2012). *CrystalExplorer*. University of Western Australia.

Zaini, M. F., Arshad, S., Thanigaimani, K., Khalib, N. C., Zainuri, D. A., Abdullah, M. & Razak, I. A. (2019). *J. Mol. Struct.* **1195**, 606–619.

Zaini, M. F., Razak, I. A., Khairul, W. M. & Arshad, S. (2018). *Acta Cryst.* E**74**, 1589–1594.

Zaini, M. F., Razak, I. A., Khairul, W. M. & Arshad, S. (2019). *Acta Cryst.* E**75**, 685–689.

Zainuri, D. A., Razak, I. A. & Arshad, S. (2018). *Acta Cryst.* E**74**, 1302–1308.

Zhuang, C., Zhang, W., Sheng, C., Zhang, W., Xing, C. & Miao, Z. (2017). *Chem. Rev.* **117**, 7762–7810

supporting information

Acta Cryst. (2020). E**76**, 387-391 [https://doi.org/10.1107/S2056989020002054]

Structural, Hirshfeld and DFT studies of conjugated *D*–π–*A* carbazole chalcone crystal

Muhamad Fikri Zaini, Ibrahim Abdul Razak, Wan Mohd Khairul and Suhana Arshad

Computing details

Data collection: *APEX2* (Bruker 2015); cell refinement: *SAINT* (Bruker 2015); data reduction: *SAINT* (Bruker 2015); program(s) used to solve structure: *SHELXS97* (Sheldrick, 2008); program(s) used to refine structure: *SHELXL2014* (Sheldrick, 2015); molecular graphics: *SHELXTL* (Sheldrick, 2008), *Mercury* (Macrae *et al.*, 2020); software used to prepare material for publication: *SHELXTL* (Sheldrick, 2008).

(*E*)-3-[4-(9,9a-Dihydro-8a*H*-carbazol-9-yl)phenyl]-1-(4-nitrophenyl)prop-2-en-1-one

Crystal data

$C_{27}H_{18}N_2O_3$
M_r = 418.43
Monoclinic, *Cc*
a = 9.9690 (5) Å
b = 24.8828 (15) Å
c = 8.3049 (4) Å
β = 94.356 (1)°
V = 2054.13 (19) Å^3
Z = 4
F(000) = 872
D_x = 1.353 Mg m^{-3}
Mo *Kα* radiation, *λ* = 0.71073 Å
Cell parameters from 9847 reflections
θ = 2.2–29.5°
μ = 0.09 mm^{-1}
T = 293 K
Block, orange
0.54 × 0.38 × 0.23 mm

Data collection

Bruker APEXII CCD diffractometer
φ and *ω* scans
Absorption correction: multi-scan (SADABS; Bruker 2015)
T_{min} = 0.783, T_{max} = 0.942
39335 measured reflections
5995 independent reflections
5046 reflections with $I > 2\sigma(I)$
R_{int} = 0.033
θ_{max} = 30.0°, θ_{min} = 1.6°
h = −13→14
k = −34→34
l = −11→11

Refinement

Refinement on F^2
Least-squares matrix: full
$R[F^2 > 2\sigma(F^2)]$ = 0.041
$wR(F^2)$ = 0.114
S = 1.03
5995 reflections
289 parameters
2 restraints
Hydrogen site location: inferred from neighbouring sites
H-atom parameters constrained
$w = 1/[\sigma^2(F_o^2) + (0.0576P)^2 + 0.455P]$ where $P = (F_o^2 + 2F_c^2)/3$
$(\Delta/\sigma)_{max} < 0.001$
$\Delta\rho_{max}$ = 0.19 e Å^{-3}
$\Delta\rho_{min}$ = −0.15 e Å^{-3}
Absolute structure: Flack *x* determined using 2241 quotients $[(I^+)-(I^-)]/[(I^+)+(I^-)]$ (Parsons et al., 2013)
Absolute structure parameter: −0.1 (3)

Special details

Experimental. The following wavelength and cell were deduced by SADABS from the direction cosines etc. They are given here for emergency use only: CELL 0.71074 8.313 9.985 13.418 68.212 88.424 85.648

Geometry. All esds (except the esd in the dihedral angle between two l.s. planes) are estimated using the full covariance matrix. The cell esds are taken into account individually in the estimation of esds in distances, angles and torsion angles; correlations between esds in cell parameters are only used when they are defined by crystal symmetry. An approximate (isotropic) treatment of cell esds is used for estimating esds involving l.s. planes.

Fractional atomic coordinates and isotropic or equivalent isotropic displacement parameters (Å²)

	x	*y*	*z*	U_{iso}*/U_{eq}
O1	0.2822 (2)	0.52900 (7)	0.1628 (3)	0.0715 (6)
O2	0.0014 (2)	0.71634 (9)	−0.3674 (2)	0.0685 (5)
O3	0.1029 (2)	0.77955 (9)	−0.2279 (3)	0.0681 (5)
N1	0.7901 (2)	0.62943 (8)	0.9806 (2)	0.0491 (4)
N2	0.0790 (2)	0.73213 (9)	−0.2556 (2)	0.0514 (5)
C1	0.8488 (2)	0.59669 (10)	1.1043 (3)	0.0494 (5)
C2	0.8433 (3)	0.54134 (11)	1.1238 (3)	0.0640 (7)
H2A	0.7917	0.5198	1.0514	0.077*
C3	0.9176 (4)	0.51939 (13)	1.2555 (4)	0.0768 (9)
H3A	0.9161	0.4824	1.2707	0.092*
C4	0.9943 (4)	0.55101 (14)	1.3656 (4)	0.0748 (9)
H4A	1.0435	0.5349	1.4522	0.090*
C5	0.9978 (3)	0.60597 (13)	1.3474 (3)	0.0633 (7)
H5A	1.0484	0.6272	1.4215	0.076*
C6	0.9240 (2)	0.62937 (10)	1.2159 (3)	0.0482 (5)
C7	0.9091 (2)	0.68404 (10)	1.1603 (3)	0.0462 (5)
C8	0.9545 (3)	0.73328 (11)	1.2227 (3)	0.0574 (6)
H8A	1.0090	0.7348	1.3185	0.069*
C9	0.9177 (3)	0.77957 (11)	1.1410 (4)	0.0644 (7)
H9A	0.9483	0.8126	1.1815	0.077*
C10	0.8351 (3)	0.77768 (11)	0.9983 (4)	0.0615 (6)
H10A	0.8106	0.8096	0.9459	0.074*
C11	0.7885 (3)	0.72941 (10)	0.9322 (3)	0.0538 (6)
H11A	0.7340	0.7284	0.8362	0.065*
C12	0.8262 (2)	0.68269 (9)	1.0148 (3)	0.0447 (4)
C13	0.7077 (2)	0.61190 (9)	0.8430 (3)	0.0467 (5)
C14	0.5978 (3)	0.57950 (11)	0.8617 (3)	0.0565 (6)
H14A	0.5780	0.5685	0.9643	0.068*
C15	0.5166 (3)	0.56331 (11)	0.7274 (3)	0.0558 (6)
H15A	0.4435	0.5410	0.7407	0.067*
C16	0.5429 (2)	0.58002 (9)	0.5731 (3)	0.0481 (5)
C17	0.6564 (2)	0.61148 (10)	0.5552 (3)	0.0511 (5)
H17A	0.6774	0.6219	0.4525	0.061*
C18	0.7384 (2)	0.62741 (10)	0.6890 (3)	0.0503 (5)
H18A	0.8139	0.6485	0.6758	0.060*
C19	0.4473 (3)	0.56599 (10)	0.4358 (3)	0.0528 (5)
H19A	0.3907	0.5369	0.4499	0.063*

C20	0.4339 (3)	0.59058 (10)	0.2947 (3)	0.0538 (6)
H20A	0.4922	0.6184	0.2730	0.065*
C21	0.3268 (2)	0.57442 (10)	0.1701 (3)	0.0511 (5)
C22	0.2696 (2)	0.61668 (10)	0.0544 (3)	0.0458 (5)
C23	0.1803 (3)	0.60042 (11)	−0.0741 (3)	0.0568 (6)
H23A	0.1623	0.5641	−0.0904	0.068*
C24	0.1188 (2)	0.63807 (11)	−0.1771 (3)	0.0550 (6)
H24A	0.0601	0.6275	−0.2637	0.066*
C25	0.1462 (2)	0.69147 (10)	−0.1489 (3)	0.0452 (5)
C26	0.2350 (2)	0.70923 (10)	−0.0246 (3)	0.0510 (5)
H26A	0.2522	0.7457	−0.0089	0.061*
C27	0.2975 (3)	0.67082 (10)	0.0758 (3)	0.0518 (5)
H27A	0.3593	0.6816	0.1590	0.062*

Atomic displacement parameters (Å²)

	U^{11}	U^{22}	U^{33}	U^{12}	U^{13}	U^{23}
O1	0.0810 (13)	0.0456 (9)	0.0816 (13)	0.0062 (9)	−0.0343 (10)	−0.0086 (9)
O2	0.0650 (11)	0.0839 (14)	0.0528 (10)	0.0021 (10)	−0.0193 (8)	0.0097 (9)
O3	0.0688 (12)	0.0606 (11)	0.0728 (12)	0.0061 (9)	−0.0075 (9)	0.0078 (9)
N1	0.0542 (11)	0.0498 (10)	0.0410 (9)	−0.0063 (8)	−0.0105 (8)	−0.0006 (8)
N2	0.0444 (10)	0.0643 (13)	0.0449 (9)	0.0046 (9)	−0.0001 (8)	0.0055 (8)
C1	0.0538 (13)	0.0540 (12)	0.0393 (10)	−0.0010 (10)	−0.0041 (9)	0.0003 (9)
C2	0.0829 (19)	0.0556 (14)	0.0521 (14)	−0.0008 (13)	−0.0045 (13)	0.0000 (11)
C3	0.110 (3)	0.0587 (16)	0.0597 (16)	0.0113 (16)	−0.0051 (16)	0.0112 (13)
C4	0.093 (2)	0.0776 (19)	0.0507 (14)	0.0152 (17)	−0.0109 (14)	0.0122 (13)
C5	0.0670 (16)	0.0815 (19)	0.0394 (11)	0.0020 (14)	−0.0092 (10)	−0.0001 (12)
C6	0.0484 (11)	0.0582 (13)	0.0375 (10)	−0.0017 (10)	−0.0005 (8)	−0.0012 (9)
C7	0.0419 (10)	0.0578 (13)	0.0386 (10)	−0.0064 (9)	0.0017 (8)	−0.0025 (9)
C8	0.0582 (14)	0.0679 (15)	0.0461 (12)	−0.0185 (12)	0.0054 (10)	−0.0105 (11)
C9	0.0772 (18)	0.0560 (15)	0.0621 (16)	−0.0218 (13)	0.0188 (14)	−0.0103 (12)
C10	0.0718 (17)	0.0531 (13)	0.0609 (15)	−0.0049 (12)	0.0137 (13)	0.0060 (11)
C11	0.0555 (13)	0.0565 (14)	0.0491 (12)	0.0000 (10)	0.0014 (10)	0.0046 (10)
C12	0.0421 (10)	0.0514 (12)	0.0401 (10)	−0.0052 (8)	−0.0003 (8)	−0.0017 (8)
C13	0.0477 (11)	0.0486 (11)	0.0417 (10)	−0.0030 (9)	−0.0096 (8)	−0.0028 (9)
C14	0.0618 (14)	0.0628 (15)	0.0436 (11)	−0.0136 (11)	−0.0051 (10)	0.0017 (10)
C15	0.0591 (14)	0.0527 (13)	0.0536 (12)	−0.0166 (11)	−0.0089 (10)	0.0029 (10)
C16	0.0539 (12)	0.0419 (10)	0.0459 (10)	0.0017 (9)	−0.0129 (9)	−0.0031 (8)
C17	0.0518 (12)	0.0587 (13)	0.0413 (10)	0.0008 (10)	−0.0064 (9)	0.0017 (9)
C18	0.0454 (11)	0.0587 (13)	0.0454 (11)	−0.0056 (10)	−0.0070 (9)	0.0029 (9)
C19	0.0589 (13)	0.0424 (11)	0.0541 (13)	−0.0001 (9)	−0.0154 (11)	−0.0054 (9)
C20	0.0541 (13)	0.0522 (13)	0.0518 (12)	0.0028 (10)	−0.0176 (10)	−0.0065 (10)
C21	0.0525 (12)	0.0490 (12)	0.0490 (12)	0.0100 (9)	−0.0150 (9)	−0.0099 (9)
C22	0.0441 (11)	0.0494 (11)	0.0419 (10)	0.0043 (9)	−0.0099 (8)	−0.0067 (8)
C23	0.0559 (13)	0.0528 (13)	0.0579 (13)	0.0003 (10)	−0.0212 (11)	−0.0102 (10)
C24	0.0516 (13)	0.0597 (14)	0.0504 (12)	0.0011 (10)	−0.0188 (10)	−0.0065 (10)
C25	0.0398 (10)	0.0572 (12)	0.0380 (9)	0.0029 (9)	−0.0022 (8)	0.0008 (9)
C26	0.0561 (13)	0.0532 (12)	0.0419 (11)	−0.0033 (10)	−0.0086 (9)	−0.0021 (9)

C27	0.0566 (13)	0.0550 (13)	0.0412 (10)	−0.0018 (10)	−0.0131 (9)	−0.0071 (9)

Geometric parameters (Å, º)

O1—C21	1.215 (3)	C11—H11A	0.9300
O2—N2	1.227 (3)	C13—C14	1.378 (4)
O3—N2	1.222 (3)	C13—C18	1.393 (3)
N1—C12	1.397 (3)	C14—C15	1.387 (3)
N1—C1	1.404 (3)	C14—H14A	0.9300
N1—C13	1.425 (3)	C15—C16	1.391 (3)
N2—C25	1.472 (3)	C15—H15A	0.9300
C1—C2	1.388 (4)	C16—C17	1.394 (4)
C1—C6	1.406 (3)	C16—C19	1.471 (3)
C2—C3	1.386 (4)	C17—C18	1.386 (3)
C2—H2A	0.9300	C17—H17A	0.9300
C3—C4	1.390 (5)	C18—H18A	0.9300
C3—H3A	0.9300	C19—C20	1.320 (3)
C4—C5	1.377 (5)	C19—H19A	0.9300
C4—H4A	0.9300	C20—C21	1.485 (3)
C5—C6	1.396 (3)	C20—H20A	0.9300
C5—H5A	0.9300	C21—C22	1.507 (3)
C6—C7	1.441 (3)	C22—C27	1.384 (3)
C7—C8	1.392 (3)	C22—C23	1.397 (3)
C7—C12	1.412 (3)	C23—C24	1.381 (3)
C8—C9	1.373 (4)	C23—H23A	0.9300
C8—H8A	0.9300	C24—C25	1.373 (4)
C9—C10	1.392 (4)	C24—H24A	0.9300
C9—H9A	0.9300	C25—C26	1.380 (3)
C10—C11	1.386 (4)	C26—C27	1.385 (3)
C10—H10A	0.9300	C26—H26A	0.9300
C11—C12	1.387 (3)	C27—H27A	0.9300
C12—N1—C1	108.39 (18)	C18—C13—N1	119.9 (2)
C12—N1—C13	125.30 (19)	C13—C14—C15	120.0 (2)
C1—N1—C13	126.31 (19)	C13—C14—H14A	120.0
O3—N2—O2	123.6 (2)	C15—C14—H14A	120.0
O3—N2—C25	118.5 (2)	C14—C15—C16	121.0 (2)
O2—N2—C25	117.9 (2)	C14—C15—H15A	119.5
C2—C1—N1	130.1 (2)	C16—C15—H15A	119.5
C2—C1—C6	121.4 (2)	C15—C16—C17	118.5 (2)
N1—C1—C6	108.6 (2)	C15—C16—C19	119.1 (2)
C3—C2—C1	117.4 (3)	C17—C16—C19	122.3 (2)
C3—C2—H2A	121.3	C18—C17—C16	120.6 (2)
C1—C2—H2A	121.3	C18—C17—H17A	119.7
C2—C3—C4	122.0 (3)	C16—C17—H17A	119.7
C2—C3—H3A	119.0	C17—C18—C13	120.0 (2)
C4—C3—H3A	119.0	C17—C18—H18A	120.0
C5—C4—C3	120.5 (3)	C13—C18—H18A	120.0

C5—C4—H4A	119.8	C20—C19—C16	126.4 (2)
C3—C4—H4A	119.8	C20—C19—H19A	116.8
C4—C5—C6	118.9 (3)	C16—C19—H19A	116.8
C4—C5—H5A	120.5	C19—C20—C21	120.8 (2)
C6—C5—H5A	120.5	C19—C20—H20A	119.6
C5—C6—C1	119.8 (2)	C21—C20—H20A	119.6
C5—C6—C7	132.8 (2)	O1—C21—C20	121.9 (2)
C1—C6—C7	107.34 (19)	O1—C21—C22	119.9 (2)
C8—C7—C12	119.5 (2)	C20—C21—C22	118.2 (2)
C8—C7—C6	133.6 (2)	C27—C22—C23	119.3 (2)
C12—C7—C6	106.9 (2)	C27—C22—C21	122.34 (19)
C9—C8—C7	119.2 (2)	C23—C22—C21	118.3 (2)
C9—C8—H8A	120.4	C24—C23—C22	120.3 (2)
C7—C8—H8A	120.4	C24—C23—H23A	119.9
C8—C9—C10	120.7 (2)	C22—C23—H23A	119.9
C8—C9—H9A	119.6	C25—C24—C23	118.5 (2)
C10—C9—H9A	119.6	C25—C24—H24A	120.7
C11—C10—C9	121.7 (3)	C23—C24—H24A	120.7
C11—C10—H10A	119.2	C24—C25—C26	123.1 (2)
C9—C10—H10A	119.2	C24—C25—N2	119.1 (2)
C10—C11—C12	117.4 (2)	C26—C25—N2	117.8 (2)
C10—C11—H11A	121.3	C25—C26—C27	117.6 (2)
C12—C11—H11A	121.3	C25—C26—H26A	121.2
C11—C12—N1	129.7 (2)	C27—C26—H26A	121.2
C11—C12—C7	121.5 (2)	C22—C27—C26	121.2 (2)
N1—C12—C7	108.8 (2)	C22—C27—H27A	119.4
C14—C13—C18	119.8 (2)	C26—C27—H27A	119.4
C14—C13—N1	120.3 (2)		

C12—N1—C1—C2	−179.4 (3)	C12—N1—C13—C18	52.0 (3)
C13—N1—C1—C2	0.6 (4)	C1—N1—C13—C18	−128.0 (3)
C12—N1—C1—C6	−0.9 (3)	C18—C13—C14—C15	−1.3 (4)
C13—N1—C1—C6	179.1 (2)	N1—C13—C14—C15	178.9 (2)
N1—C1—C2—C3	176.8 (3)	C13—C14—C15—C16	−1.1 (4)
C6—C1—C2—C3	−1.6 (4)	C14—C15—C16—C17	2.9 (4)
C1—C2—C3—C4	0.5 (5)	C14—C15—C16—C19	−174.4 (2)
C2—C3—C4—C5	0.5 (6)	C15—C16—C17—C18	−2.4 (4)
C3—C4—C5—C6	−0.5 (5)	C19—C16—C17—C18	174.9 (2)
C4—C5—C6—C1	−0.5 (4)	C16—C17—C18—C13	0.1 (4)
C4—C5—C6—C7	−178.0 (3)	C14—C13—C18—C17	1.8 (4)
C2—C1—C6—C5	1.5 (4)	N1—C13—C18—C17	−178.4 (2)
N1—C1—C6—C5	−177.1 (2)	C15—C16—C19—C20	158.6 (3)
C2—C1—C6—C7	179.7 (2)	C17—C16—C19—C20	−18.7 (4)
N1—C1—C6—C7	1.1 (3)	C16—C19—C20—C21	−175.9 (2)
C5—C6—C7—C8	−5.4 (5)	C19—C20—C21—O1	−27.7 (4)
C1—C6—C7—C8	176.8 (3)	C19—C20—C21—C22	150.0 (2)
C5—C6—C7—C12	177.0 (3)	O1—C21—C22—C27	167.4 (3)
C1—C6—C7—C12	−0.8 (2)	C20—C21—C22—C27	−10.4 (3)

C12—C7—C8—C9	−0.1 (3)	O1—C21—C22—C23	−9.5 (4)
C6—C7—C8—C9	−177.5 (3)	C20—C21—C22—C23	172.7 (2)
C7—C8—C9—C10	0.6 (4)	C27—C22—C23—C24	−1.1 (4)
C8—C9—C10—C11	−0.8 (4)	C21—C22—C23—C24	175.9 (2)
C9—C10—C11—C12	0.6 (4)	C22—C23—C24—C25	−0.8 (4)
C10—C11—C12—N1	177.0 (2)	C23—C24—C25—C26	1.7 (4)
C10—C11—C12—C7	−0.1 (3)	C23—C24—C25—N2	−178.7 (2)
C1—N1—C12—C11	−177.0 (2)	O3—N2—C25—C24	179.1 (2)
C13—N1—C12—C11	3.0 (4)	O2—N2—C25—C24	−0.6 (3)
C1—N1—C12—C7	0.4 (2)	O3—N2—C25—C26	−1.3 (3)
C13—N1—C12—C7	−179.6 (2)	O2—N2—C25—C26	179.0 (2)
C8—C7—C12—C11	−0.1 (3)	C24—C25—C26—C27	−0.6 (4)
C6—C7—C12—C11	177.9 (2)	N2—C25—C26—C27	179.7 (2)
C8—C7—C12—N1	−177.8 (2)	C23—C22—C27—C26	2.3 (4)
C6—C7—C12—N1	0.2 (2)	C21—C22—C27—C26	−174.6 (2)
C12—N1—C13—C14	−128.2 (3)	C25—C26—C27—C22	−1.4 (4)
C1—N1—C13—C14	51.8 (4)		

Hydrogen-bond geometry (Å, º)

*Cg*4 is the centroid of the C13–C18 ring.

D—H···*A*	*D*—H	H···*A*	*D*···*A*	*D*—H···*A*
C15—H15*A*···O1^{i}	0.93	2.42	3.291 (3)	155
C18—H18*A*···O2^{ii}	0.93	2.56	3.490 (3)	173
C9—H9*A*···*Cg*4^{iii}	0.93	2.89	3.758 (3)	155

Symmetry codes: (i) *x*, −*y*+1, *z*+1/2; (ii) *x*+1, *y*, *z*+1; (iii) *x*+1/2, −*y*+3/2, *z*+1/2.